Petrology, Vol. 3, No. 6, 1995, pp. 511 - 524. Translated from Petrologiya, Vol. 3, No. 6, 1995, pp. 562 - 576.

Garnet–Cordierite Metapelites of the Voronezh Massif: Thermal Evolution and Cooling Rate

V. Yu. Gerasimov* and K. A. Savko**

**Institute of the Geology of Ore Deposits, Petrography, Mineralogy, and Geochemistry, Russian Academy of Sciences, Staromonetnyi per. 35, Moscow, 109017 Russia*

***Voronezhgeologiya Geologic–Geophysical Survey, ul. Begovaya 205, Voronezh, 349016 Russia*

Received April 22, 1994

Abstract – Detailed microprobe studies of rock-forming minerals from the high-temperature Voronezh metapelites reveal a two-component diffusion zoning in garnet grains near their contacts with biotite and cordierite. The zoning was formed by the diffusion counterflows of iron and magnesium. The initial chemistries of the minerals and the metamorphic P–T conditions were computed using the model for nonequilibrium diffusion mass exchange (for a closed system). The rate of the metamorphic temperature evolution was evaluated on the basis of diffusion-induced concentration profiles in the garnet. During the retrograde stage, starting from a temperature of 670°C, the metamorphic complex cooled at the rate of 3°C/Ma under a pressure of no more than 4 kbar and an uplift rate of 0.03 km/Ma.

INTRODUCTION

Mineral equilibria are traditionally used to reconstruct thermodynamic and geodynamic regimes that occurred in the earth crust (Perchuk, 1970). However, studies of mineral assemblages with zoned minerals are confronted with certain difficulties, because the chemical heterogeneities of the phases contradict the notion that the chemical potentials of their components must equilibrate with the onset of thermodynamic equilibrium.

Diffusion zoning in garnet and some other minerals normally forms at the contacts of mineral grains due to a nonequilibrium component redistribution during a retrograde metamorphic stage. The development of such zoning is controlled by the low rates of volume diffusion in the mineral lattices. The occurrence of diffusion zoning indicates that the petrologic system departed from its equilibrium state, the relaxation rate of the system became lower than the evolution rates of its intensive parameters, and the system closed at a certain moment (Dodson, 1973). Kinetic models for such transitional states, developed in application to mineralogical thermobarometry, are referred to as *geospeedometry* (Lasaga, 1983). Here, we mean the examination of mineral reaction reversibility during retrograde metamorphic stages, when thermobarometric data are dependent on the cooling rate of the system (Gerasimov, 1992). In this case, the diffusion zoning can be used as a natural thermochronometer to compute the rate and duration of the temperature evolution as well as the extent to which the mineral assemblage was in equilibrium.

This paper is devoted to the petrologic studies of metamorphic rocks from the Russian Platform basement within the boundaries of the Voronezh Anteclise. Some of the obtained values and geodynamic interpretations are admittedly tentative, and should be considered as preliminary until comprehensive thermochronological studies, including isotopic, are performed.

GEOLOGIC SETTING

The Early Proterozoic metapelites of the Vorontsovskii Group (Savko, 1991) are situated in the eastern portion of the Voronezh Massif. The massif has a complicated block structure, and is a southeastern fragment of the Russian Platform basement (Fig. 1). The metapelites occur over an area of 70 000 km^2 and are ubiquitously overlain by a sedimentary cover more than 80 m thick. They are intruded by numerous ultrabasite, gabbrodolerite, diorite, and granite bodies, and syenite dikes. Earlier studies revealed a metamorphic zonation of the Vorontsovskii Group. The zonation is of a low-depth type (Savko, 1991), and grades from the andalusite–staurolite zone to the sillimanite–potassium feldspar–cordierite zone with increasing temperature.

Figure 2 presents fragments of this temperature zonation and the boundaries of the metamorphic zones: (1) the sillimanite isograde, which separates the staurolite–sillimanite and the andalusite–staurolite zones; (2) the staurolite-out isograde, which indicates the onset of the muscovite–sillimanite zone; (3) the muscovite-out isograde ($Ms + Qtz = Sil + Kfs$), which marks the transition to the sillimanite–potassium feldspar–cordierite zone. The biotite–sillimanite assemblage decomposes and produces cordierite rims almost simultaneously with the disappearance of muscovite. Cordierite rims also crystallize between garnet and sillimanite grains and, hence, the mineral equilibria of the sillimanite–potassium feldspar–cordierite zone corre-

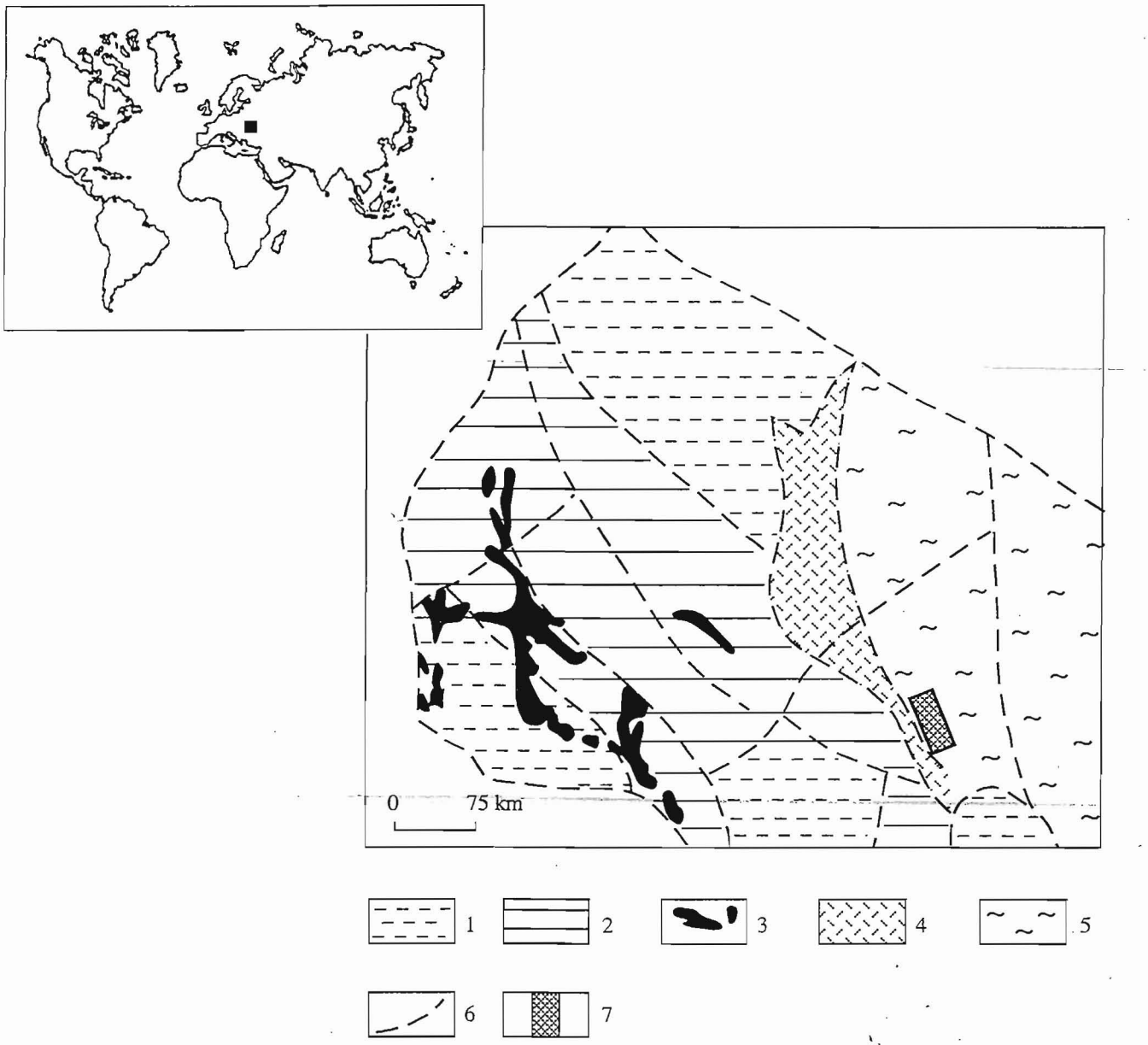

Fig. 1. Schematic tectonic map of the Vozonezh Massif.
1 – Protoplatform Archean blocks; 2 – Kursk Magnetic Anomaly Megablock; 3 – Upper Archean greenstone belts; 4 – Voronezh Block; 5 – eastern Voronezh Massif; 6 – deep faults; 7 – study area.
The solid rectangle in the inset indicates the study area.

spond to the conditions that are transitional from the biotite–sillimanite to the garnet–cordierite–potassium-feldspar facies (Korikovskii, 1979). All of the samples with the most informative mineral assemblages of these zones were obtained from the drill core near the Podkolodnovskii nickel deposit (Fig. 2).

PETROGRAPHY

The metapelites are medium-grained biotite–sillimanite gneisses with cordierite and, more seldom, garnet and potassium feldspar. Garnet grains are 1 to 2 mm across, normally anhendral; they are often resorbed by biotite and surrounded by cordierite rims. Low-temperature transformations are weak: the cordierite is incidentally pinitized, and the biotite is replaced somewhere by secondary chlorite and muscovite.

Sample 6958/391 contains a typical metapelite mineral assemblage of the Vorontsovskii Group (PR_1vc): *Grt + Bt + Crd + Sil + Qtz + (Spl) + Pl*. Figure 3 demonstrates a thin section fragment with the loci of mineral microprobe analyses; the mineral chemistries and cation proportions are listed in Tables 1 - 4. The garnet contains inclusions of biotite, quartz, plagioclase, and

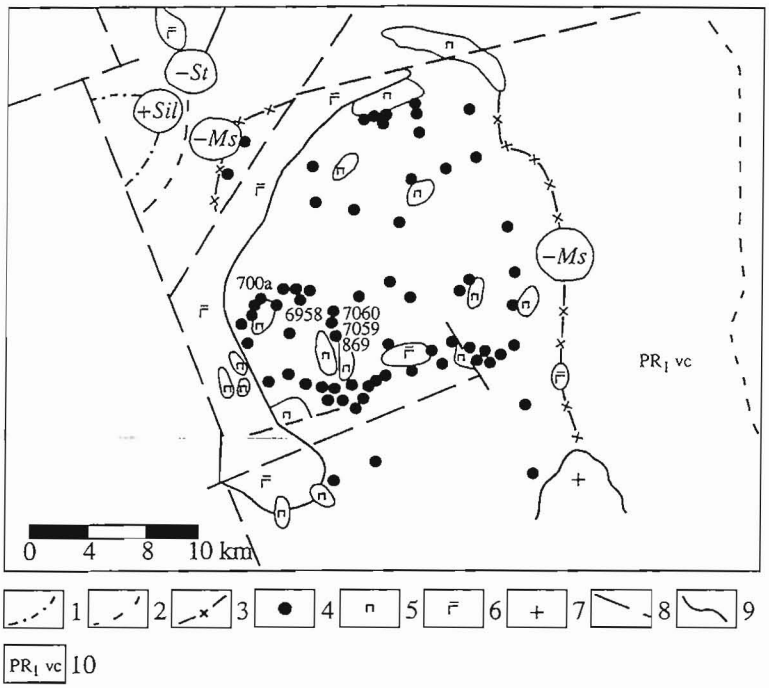

Fig. 2. Metamorphic zonation of the study area (Savko, 1991).
1 - 3 – isograde: 1 – sillimanite (low-temperature staurolite–sillimanite zone), 2 – staurolite-out isograde (low-temperature muscovite–sillimanite zone), 3 – muscovite-out isograde (low-temperature sillimanite–potassium feldspar–cordierite zone); 4 – sampling localities in boreholes (numbers are given for chemically examined samples); 5 - 7 – intrusive rocks: 5 – peridotite, 6 – gabbronorite, 7 – granite; 8 – faults; 9 – geologic boundaries; 10 – Vorontsovskii Group index.

sillimanite, and is partly rimmed by cordierite. The cordierite sometimes bears clusters of small isolated grains of ferrous spinel, which contains up to 5 wt % ZnO, a fact indicating that the rock had contained Zn-bearing staurolite. Its complete decomposition occurred according to the reaction:

$$St = Crd + Spl + Sil + H_2O \quad (I)$$

at a temperature of 600°C (Korikovskii, 1979). A further temperature increase in this aureole led to the formation of cordierite rims, which crystallized first between the sillimanite and biotite, and then around the garnet. The latter reaction proceeds with the decomposition of sillimanite and quartz:

$$Crt + Sil + Qtz = Crd. \quad (II)$$

This was thoroughly studied experimentally (Aranovich and Podlesskii, 1982) and is traditionally employed as a reliable geobarometer (Marakushev, 1965; Perchuk, 1970; Perchuk *et al.*, 1983). The evolution of mineral assemblages in the Vorontsovskii metapelites during prograde metamorphism can be illustrated by a (Mg, Fe)–Al–Si diagram (Figs. 4 and 5).

REGULARITIES IN THE EVOLUTION OF THE MINERAL CHEMISTRIES

In order to determine the extent to which the minerals are in equilibrium in their assemblage, we performed a detailed microprobe examination of the minerals in thin sections. Diffusion zones in the garnet margins near contacts with biotite and cordierite were the most thoroughly studied. Zones of diffusion mass exchange between minerals are controlled by a nonequilibrium Fe-Mg exchange reaction during the retrograde metamorphic stages, and indicate that concentration gradients and counterdiffusion flows of these elements appeared. The scale on which the mass exchange occurs is indicative of the reversibility of the mineral equilibria and is controlled, to a first approximation, by the cooling rate of the system (Gerasimov, 1992).

In addition to the individual analyses in Sample 6958/391, we measured three continuous concentration profiles with the steps of 2 and 3 μ across the boundaries between the minerals (Fig. 6). These profiles show a clear diffusion zoning with the concentrations varying over wide limits. The zoning is well preserved in the garnet, but is less clear in the biotite. Apparently, reliable thermobarometric estimates should be based only on the equilibrium compositions selected from wide spectra of the mineral chemistries.

Let us consider the evolution of the mineral system more thoroughly. The garnet grain is approximately 2000 μm in diameter; its central portion is nearly homogeneous with the Mg mole fraction at 0.18 ± 0.01 and constant concentrations of CaO and MnO of approximately 1 wt %. Such a structure is fairly typical of granulitelike mineral assemblages, in which the primary growth zoning is usually obliterated at temperatures

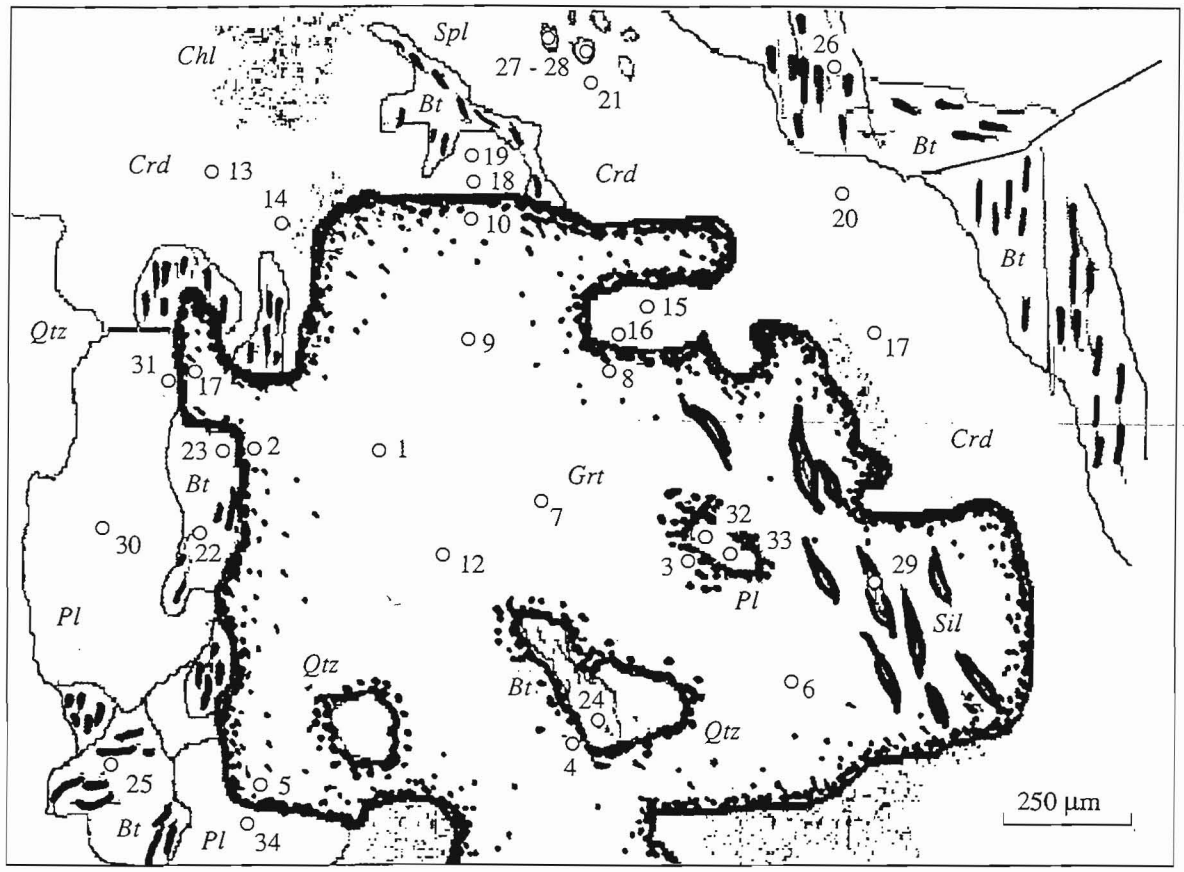

Fig. 3. Sketch showing Sample 6958/391 (portion of a thin section) with loci of microprobe analyses (Tables 1 - 4).
Mineral symbols: *Bt* – biotite, *Chl* – chlorite, *Crd* – cordierite, *Grt* – garnet, *Pl* – plagioclase, *Qtz* – quartz, *Sil* – sillimanite, *Spl* – spinel.

above 700°C. Diffusion zoning occurs in the garnet only at contacts with other iron-magnesium silicates (including those in inclusions). The zones are 100 - 120 μm thick. The magnesium mole fraction of the garnet strongly decreases (from 0.18 to 0.09) rimward, whereas these values of the adjacent biotite and cordierite increase to the maximum. Concentration profiles across the diffusion zones are well approximated by an exponential function whose plots approach, asymptotically, the concentration axis.

In order to test the stoichiometric nature of the garnet crystalline solution, we plotted the garnet compositions from the diffusion zone in a correlation diagram in terms *Prp–Alm* (Fig. 7). The plot evidently demonstrates a clear negative linear correlation between the contents of the almandine and pyrope components (correlation coefficient $R = 0.98$, the proportion ratio is –1.05), a fact indicating that the diffusion process was two-component, and the iron and magnesium fluxes were counterbalanced.

The biotite and cordierite also change their chemistries due to later exchange reactions with the garnet during the retrograde metamorphic stage, with the compositional changes being stronger the smaller the grains were and the closer they were to the garnet. A biotite grain (*Bt*-26 in Table 3) in the groundmass is fairly detached from the garnet and shows almost no compositional changes; it has the minimum magnesium mole fraction (0.44) and the maximum titanium dioxide content (3.6 wt % TiO_2) – all of these features allowed us to ascribe this grain to the highest temperature. Conversely, isolated biotite inclusions in the garnet (*Bt*-24 in Table 3) have the highest magnesium mole fractions (0.55) at the same titanium content, because titanium did not participate in the later exchange reaction with the garnet. Biotite grains adjacent to the garnet grain (Fig. 3) have lower titanium contents, and their magnesium numbers depend on their sizes. For example, the titanium dioxide content of a small biotite grain (*Bt*-22 and *Bt*-23 in Table 3) is 2.8 ± 0.1 wt % at a magnesium mole fraction of 0.50 ± 0.01 (Fig. 8); the latter, however, increases to 0.55 within a narrow (10 μm) diffusion zone preserved at the contact with the garnet.

The cordierite rims show a similar tendency to increase the magnesium mole fractions toward their contacts with the garnet. The cordierite magnesium mole fraction is the lowest (0.60) at a distance of 250 - 300 μm

Table 1. Microprobe analyses and cation proportions of garnet from Sample 6958/391 (Fig. 3)

Components	1	2	3	4	5	6	7	8	9	10	11	12
SiO_2	37.32	37.23	37.59	37.33	37.63	37.49	37.29	37.13	37.62	36.99	37.01	37.29
TiO_2	0.05	0.07	0.05	0.06	0.04	0.04	0.06	0.03	0.01	0.02	0.01	0.02
Al_2O_3	20.77	21.03	20.95	21.11	21.05	21.25	21.14	20.69	20.39	20.86	20.90	21.12
Cr_2O_3	0.09	0.02	0.03	0.05	0.00	0.03	0.06	0.06	0.04	0.06	0.04	0.07
FeO	34.65	36.95	34.56	35.69	35.15	34.50	33.94	36.10	34.22	36.39	35.26	34.90
MnO	1.16	1.47	0.90	1.20	1.32	1.22	1.04	1.66	1.18	1.75	1.41	1.26
MgO	4.21	2.45	4.52	3.21	4.03	4.22	4.67	2.98	4.51	2.69	3.62	4.20
CaO	0.92	0.80	1.02	0.93	0.89	0.85	0.83	0.97	1.07	0.91	0.80	0.98
Na_2O	0.00	0.00	0.02	0.00	0.04	0.00	0.00	0.00	0.05	0.03	0.04	0.00
K_2O	0.00	0.01	0.00	0.00	0.00	0.00	0.00	0.01	0.00	0.01	0.01	0.00
$Fe_2O_3^*$	0.00	0.00	0.00	0.00	0.00	0.00	0.00	0.00	0.17	0.00	0.00	0.17
Total	99.15	100.04	99.65	99.57	100.13	99.61	99.03	99.63	99.25	99.70	99.10	100.00
Si	3.01	3.02	3.01	3.02	3.01	3.01	3.00	3.01	3.03	3.00	3.00	2.99
Ti	0.00	0.00	0.00	0.00	0.00	0.00	0.00	0.00	0.00	0.00	0.00	0.00
Al	1.98	2.01	1.98	2.01	1.99	2.01	2.01	1.98	1.94	2.00	2.00	1.99
Cr^{3+}	0.01	0.00	0.00	0.00	0.00	0.00	0.00	0.00	0.00	0.00	0.00	0.00
Fe^{3+}	0.00	0.00	0.00	0.00	0.00	0.00	0.00	0.00	0.01	0.00	0.00	0.01
Fe^{2+}	2.34	2.50	2.31	2.41	2.35	2.31	2.28	2.44	2.30	2.47	2.39	2.33
Mn	0.08	0.10	0.06	0.08	0.09	0.08	0.07	0.11	0.08	0.12	0.10	0.09
Mg	0.51	0.30	0.54	0.39	0.48	0.51	0.56	0.36	0.54	0.33	0.44	0.50
Ca	0.08	0.07	0.09	0.08	0.08	0.07	0.07	0.08	0.09	0.08	0.07	0.08
Na	0.00	0.00	0.00	0.00	0.01	0.00	0.00	0.00	0.01	0.00	0.01	0.00
K	0.00	0.00	0.00	0.00	0.00	0.00	0.00	0.00	0.00	0.00	0.00	0.00
O	12.01	12.03	12.00	12.03	12.00	12.02	12.01	12.00	12.00	12.00	12.00	11.99
Alm	0.778	0.843	0.771	0.815	0.784	0.778	0.764	0.814	0.763	0.824	0.798	0.777
Prp	0.169	0.100	0.180	0.131	0.160	0.170	0.188	0.120	0.180	0.109	0.146	0.167
Spes	0.026	0.034	0.020	0.028	0.030	0.028	0.024	0.038	0.027	0.040	0.032	0.029
Gros	0.024	0.023	0.028	0.025	0.025	0.024	0.022	0.026	0.024	0.025	0.022	0.021
Adr	0.000	0.000	0.000	0.000	0.000	0.000	0.000	0.000	0.005	0.000	0.000	0.005
Uvar	0.003	0.001	0.001	0.002	0.000	0.001	0.002	0.002	0.001	0.002	0.001	0.002
X_{Mg}	0.173	0.102	0.185	0.134	0.165	0.174	0.192	0.123	0.185	0.112	0.150	0.172

Note: Here and in Tables 2 - 4 – $X_{Mg} = Mg/(Mg + Fe + Mn)$.

(Fig. 3, *Crd*-20 in Table 2) from the garnet, and increases to 0.68 in the contact (Fig. 9).

Hence, both the relationships of the minerals in thin sections and the changes in the mineral chemistries indicate that the garnet was almost entirely homogenized at peak metamorphic conditions and partly replaced by cordierite rims, according to reaction (II). The system attained thermodynamic equilibrium, whose conditions can be estimated using the most magnesian large garnet grains and the most ferrous (relict) biotite and cordierite. During the retrograde stage, the exchange reactions

$$Grt_{Mg} + Crd_{Fe} = Grt_{Fe} + Crd_{Mg}, \quad \text{(III)}$$

$$Grt_{Mg} + Bt_{Fe} = Grt_{Fe} + Bt_{Mg} \quad \text{(IV)}$$

controlled the magnesium redistribution between the garnet and other iron-magnesium minerals in line with the principle of phase correspondence (Perchuk, 1970). The reactions became more sluggish with decreasing temperature, and the system became closed. Concen-

Table 2. Microprobe analyses and cation proportions of cordierite from Sample 6958/391 (Fig. 3)

Components	*Crd*-13	*Crd*-14	*Crd*-15	*Crd*-16	*Crd*-17	*Crd*-18	*Crd*-19	*Crd*-20	*Crd*-21
SiO_2	47.72	47.12	47.82	46.98	46.51	46.93	46.66	46.87	46.97
TiO_2	0.03	0.03	0.00	0.08	0.01	0.03	0.03	0.00	0.03
Al_2O_3	31.59	31.36	31.68	31.03	31.16	30.93	30.77	30.24	31.17
Cr_2O_3	0.00	0.00	0.00	0.00	0.03	0.05	0.03	0.06	0.00
FeO	8.82	8.32	7.53	7.38	8.37	7.56	8.23	8.76	8.55
MnO	0.08	0.16	0.10	0.11	0.06	0.02	0.13	0.14	0.17
MgO	7.63	8.20	8.45	8.66	8.01	8.21	7.68	7.43	7.77
CaO	0.00	0.00	0.00	0.00	0.00	0.00	0.00	0.00	0.00
Na_2O	0.18	0.13	0.12	0.13	0.19	0.14	0.15	0.16	0.17
K_2O	0.01	0.00	0.00	0.03	0.02	0.01	0.00	0.00	0.03
Total	96.06	95.32	95.72	94.40	94.36	93.88	93.68	93.66	94.86
Si	5.04	5.00	5.04	5.01	4.99	5.05	5.05	5.09	5.02
Ti	0.00	0.00	0.00	0.01	0.00	0.00	0.00	0.00	0.00
Al	3.93	3.92	3.94	3.90	3.94	3.92	3.92	3.87	3.92
Cr	0.00	0.00	0.00	0.00	0.00	0.00	0.00	0.01	0.00
Fe^{2+}	0.78	0.74	0.66	0.66	0.75	0.68	0.74	0.79	0.76
Mn	0.01	0.01	0.01	0.01	0.01	0.00	0.01	0.01	0.02
Mg	1.20	1.30	1.33	1.38	1.28	1.32	1.24	1.20	1.24
Ca	0.00	0.00	0.00	0.00	0.00	0.00	0.00	0.00	0.00
Na	0.04	0.03	0.02	0.03	0.04	0.03	0.03	0.03	0.04
K	0.00	0.00	0.00	0.00	0.00	0.00	0.00	0.00	0.00
O	17.99	17.95	18.00	17.96	17.93	18.00	18.00	18.01	17.96
X_{Mg}	0.605	0.633	0.664	0.673	0.629	0.659	0.621	0.598	0.614

Table 3. Microprobe analyses and cation proportions of biotite from Sample 6958/391 (Fig. 3)

Components	*Bt*-22	*Bt*-23	*Bt*-24	*Bt*-25	*Bt*-26	Components	*Bt*-22	*Bt*-23	*Bt*-24	*Bt*-25	*Bt*-26
SiO_2	36.32	36.02	34.93	35.72	35.11	Al(IV)	1.24	1.24	1.24	1.23	1.26
TiO_2	2.59	2.81	3.74	2.72	3.59	Al(VI)	0.57	0.54	0.43	0.52	0.47
Al_2O_3	20.12	19.74	17.90	19.14	18.83	Cr	0.00	0.01	0.00	0.01	0.01
Cr_2O_3	0.00	0.11	0.07	0.10	0.10	Fe^{2+}	1.14	1.13	1.05	1.17	1.29
FeO	17.90	17.67	15.90	18.01	19.76	Mn	0.00	0.00	0.00	0.00	0.00
MnO	0.00	0.02	0.01	0.01	0.02	Mg	1.15	1.16	1.29	1.15	1.02
MgO	10.11	10.17	10.95	9.93	8.76	Ca	0.00	0.00	0.00	0.00	0.00
CaO	0.00	0.00	0.00	0.00	0.00	Na	0.03	0.02	0.04	0.03	0.03
Na_2O	0.17	0.14	0.24	0.22	0.17	K	0.72	0.73	0.99	0.78	0.94
K_2O	7.43	7.51	9.84	7.93	9.41	OH	2.00	2.00	2.00	2.00	2.00
H_2O^*	4.44	4.40	3.79	4.22	3.91	H^+	0.25	0.25	0.00	0.18	0.04
Total	99.08	98.59	97.37	98.00	99.66	O	10.31	10.31	10.34	10.31	10.32
Si	2.76	2.76	2.76	2.77	2.74	X_{Mg}	0.502	0.506	0.551	0.496	0.441
Ti	0.15	0.16	0.22	0.16	0.21	X_{Na}	0.034	0.028	0.036	0.040	0.027

Note: H_2O^* is calculated from crystallochemical considerations. $X_{Na} = Na/(Na + K + Ca)$.

Table 4. Microprobe analyses and cation proportions of coexisting spinel (*Spl*), sillimanite (*Sil*), and plagioclase (*Pl*) from Sample 6958/391 (Fig. 3)

Components	*Spl*-27	*Spl*-28	*Sil*-29	*Pl*-30	*Pl*-31	*Pl*-32	*Pl*-33	*Pl*-34
SiO_2	0.07	0.08	37.58	61.82	61.33	60.61	60.94	61.80
TiO_2	0.00	0.00	0.00	0.02	0.02	0.01	0.00	0.05
Al_2O_3	57.70	56.60	57.47	23.47	23.44	24.19	24.10	22.92
Cr_2O_3	0.13	0.03	0.04	0.00	0.06	0.02	0.27	0.00
FeO	31.20	31.16	2.89	0.07	0.01	0.24	0.52	0.23
MnO	0.10	0.09	0.08	0.00	0.03	0.07	0.03	0.00
MgO	3.24	3.07	0.29	0.00	0.02	0.01	0.02	0.02
CaO	0.00	0.00	0.09	5.58	5.33	6.63	6.32	4.97
ZnO	5.03	5.17	0.00	0.00	0.00	0.01	0.02	0.00
Na_2O	0.01	0.09	0.00	8.70	8.92	8.03	8.00	9.05
K_2O	0.01	0.00	0.00	0.17	0.17	0.20	0.17	0.06
Fe_2O_3*	1.85	2.75	0.00	0.00	0.00	0.00	0.00	0.00
Total	99.33	99.05	98.46	99.83	99.33	100.02	100.39	99.10
Si	0.00	0.00	1.03	2.73	2.72	2.69	2.70	2.75
Ti	0.00	0.00	0.00	0.00	0.00	0.00	0.00	0.00
Al	1.96	1.93	1.88	1.23	1.24	1.27	1.27	1.21
Cr	0.00	0.00	0.00	0.00	0.00	0.01	0.00	0.00
Fe^{3+}	0.04	0.06	0.00	0.00	0.00	0.00	0.00	0.00
Fe^{2+}	0.75	0.75	0.07	0.00	0.00	0.01	0.02	0.01
Mn	0.00	0.00	0.00	0.00	0.00	0.00	0.00	0.00
Mg	0.14	0.13	0.01	0.00	0.00	0.00	0.00	0.00
Ca	0.00	0.00	0.00	0.27	0.26	0.32	0.30	0.24
Zn	0.11	0.11	0.00	0.00	0.00	0.00	0.00	0.00
Na	0.00	0.01	0.00	0.75	0.77	0.70	0.69	0.79
K	0.00	0.00	0.00	0.01	0.01	0.01	0.01	0.00
O	4.00	4.00	4.98	7.97	7.95	7.97	7.98	7.96
Ab				0.731	0.745	0.679	0.689	0.765
An				0.259	0.246	0.310	0.301	0.232
Or				0.009	0.009	0.011	0.010	0.003
X_{Mg}	0.16	0.15						

Note: Fe_2O_3* is recalculated according to crystallochemical considerations.

tration gradients occurred at phase boundaries, and the system departed from the state of equilibrium. Further nonequilibrium redistribution of components resulted in partial or complete changes in the mineral chemistries.

Taking into account the limitations imposed by the microprobe beam diameter (1 to 2 μm), further searches for extreme compositions that could be used to assess the minimum temperature seem to be fairly senseless. The monotonous increase in the concentration gradient toward the phase boundary indicates that the cooling was also monotonous and occurred with a finite rate during a single episode (Gerasimov, 1992).

SPECIFIC FEATURES OF THE NONISOTHERMAL DIFFUSION MODEL

In cases when the thickness of the diffusion zone is much less than the radius of the grain boundary (Fig. 3), diffusion through an isotropic crystal can be described

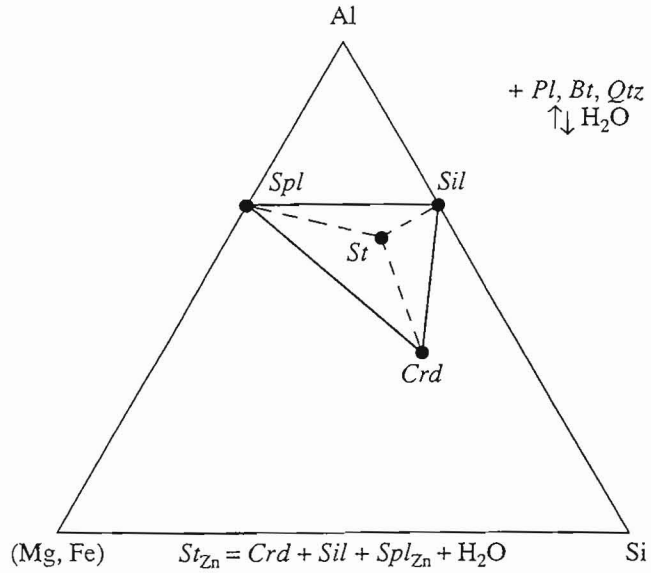

$St_{Zn} = Crd + Sil + Spl_{Zn} + H_2O$

Fig. 4. Decomposition of staurolite into cordierite, spinel, and sillimanite.

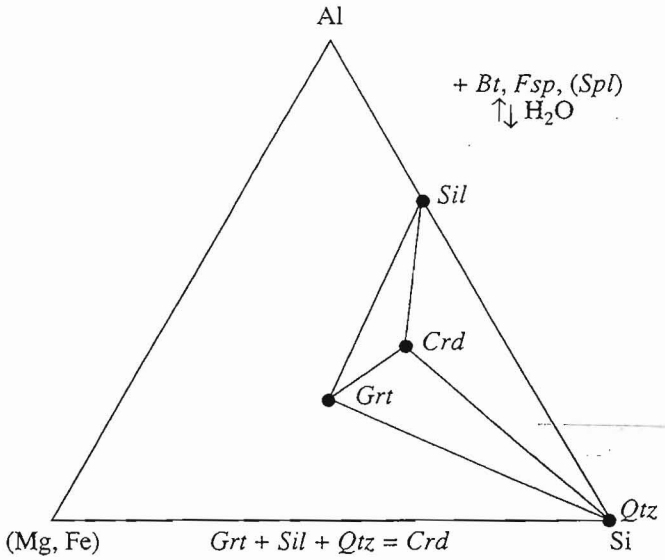

$Grt + Sil + Qtz = Crd$

Fig. 5. Replacement of garnet by cordierite.

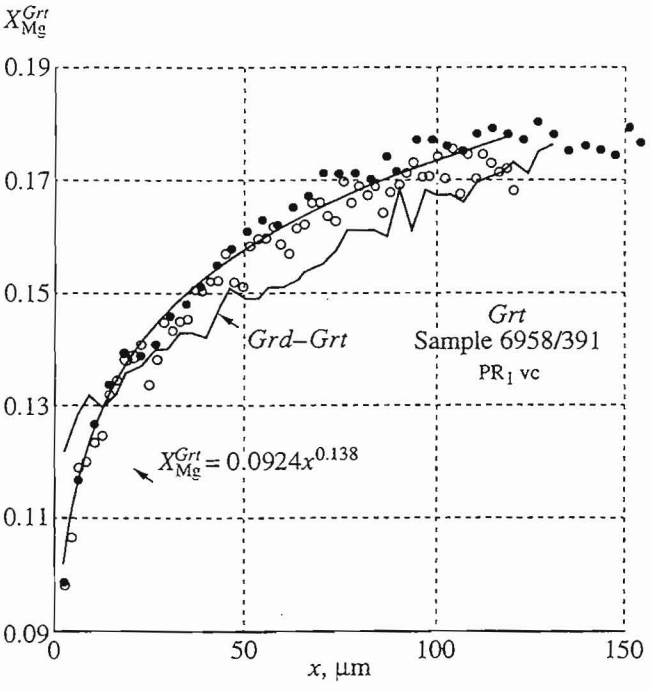

Fig. 6. Zones of diffusion mass-exchange between garnet, biotite (solid and open circles, respectively), and cordierite (polygonal line) detected by the microprobe.

The concentration distribution is well approximated by an exponential function (solid curve). The biotite contacts show stable reproducibility of the data (the fields for open and solid circles nearly coincide).

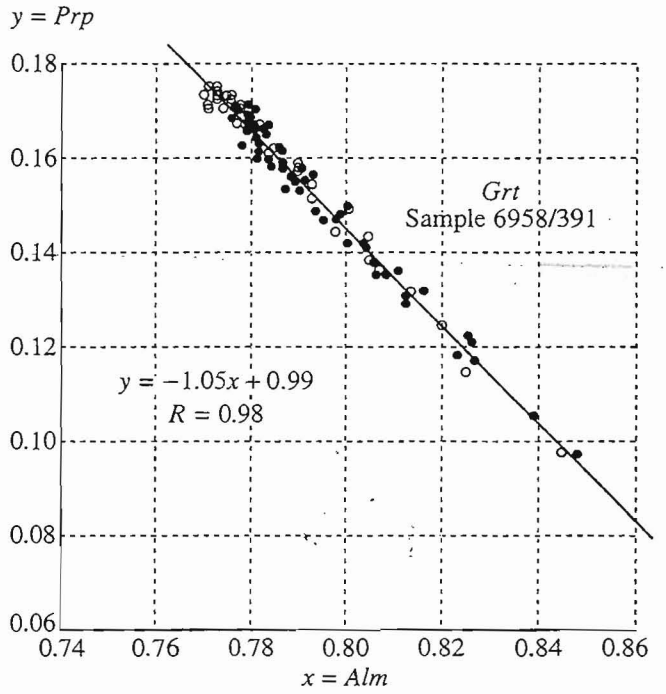

Fig. 7. Correlation between the pyrope and almandine concentrations in the garnet diffusion zone.

There is an evident negative correlation with a coefficient $R = 0.98$. Magnesium losses in each point of the profile are balanced by an iron input in accord with the solid solution stoichiometry.

by an unidimensional diffusion equation:

$$\frac{\partial c}{\partial t} = \frac{\partial}{\partial x}\left(D\frac{\partial c}{\partial x}\right).$$

The coefficient of diffusion is a function of temperature and can be expressed in the form of Arrhenius equation over a broad temperature range

$$D = D_0 \exp[-Q/(RT(t))].$$

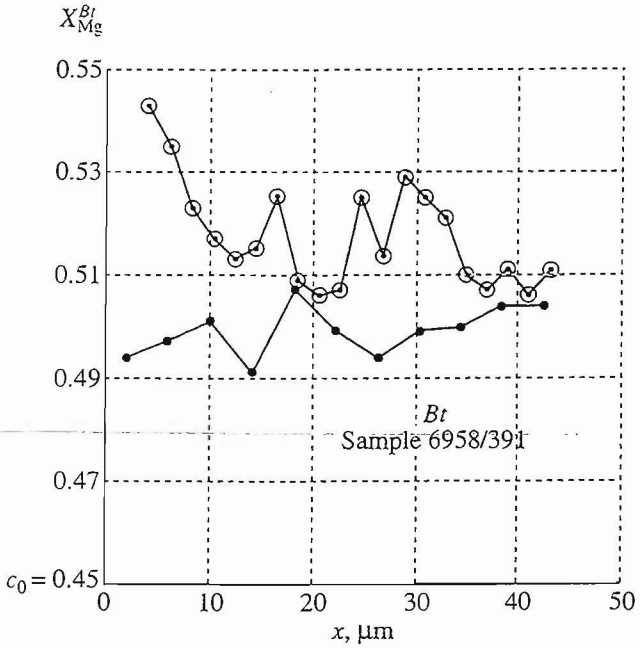

Fig. 8. Compositions (microprobe data) of biotite near contacts with garnet.
The grains are almost homogeneous or, sometimes, show a slight tendency to increase magnesium numbers toward the contacts (open circles).

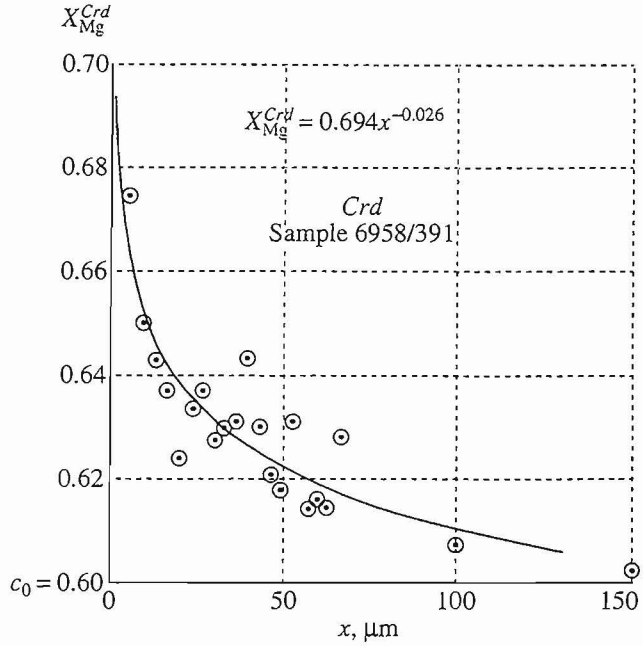

Fig. 9. Diffusion zone in cordierite at its contact with garnet. At decreasing temperature, a magnesium input is set off by iron removal. The diffusion front has shifted for 400 - 500 μm, and the concentration variations are well approximated by the function $X_{Mg}^{Crd} = 0.694x^{-0.026}$.

The temperature of a retrograde metamorphic stage is a monotonously decreasing function of time. The parameters of the Arrhenius equation can be determined experimentally [$D_0 = 1.662$ cm^2/s; the diffusion activation energy $Q = 345$ kJ/mol (Gerasimov, 1987)]. Thus, the diffusion coefficient is a complicated function of the only variable, time t, so that we can factor it outside the differential sign:

$$\frac{\partial c}{\partial t} = D(t)\frac{\partial^2 c}{\partial x^2}.$$

This equation has a solution at respective boundary and initial conditions, which are conventionally accepted in describing nonequilibrium exchange reactions (Lasaga, 1983; Gerasimov, 1992), and can be written in the form of an infinite series:

$$c(x, t') = \sum_{n=1}^{\infty} 2/(\lambda_n L)\sin(\lambda_n x)\exp(-\lambda_n^2 t')c_0$$

$$\times\left[1 + \lambda_n^2/\gamma'\exp(\lambda_n^2/\gamma')\int_0^1 \exp(-\lambda_n^2 z/\gamma')(z)^{\alpha} dz\right],$$

$$0 \le x \le L, \quad 0 \le t' \le 1/\gamma' = D^0/\gamma, \quad \gamma = Qs/(RT_0^2),$$

$$\alpha = \Delta H^0/QX_{0_{Mg}}^{Grt} = \text{const},$$

$$D^0 = D_0\exp(-Q/RT_0),$$

$$t' = D^0/\gamma[1 - \exp(-\gamma t)].$$

The concentration c in a diffusion zone is a function of the x coordinate and the new variable t'. The form of its isochronous section depends on the linear dimensions L of a garnet crystal, the exchange reaction enthalpy ΔH^0, the initial cooling rate s at the starting temperature T_0 of the nonequilibrium exchange, diffusion activation energy Q, and the preexponential factor D_0.

Before beginning the computer simulation of the diffusion zoning of our sample, let us consider some theoretical implications. The compatibility condition of the two diffusion mineral volumes necessitates the equality of mass counterflows via the interface:

$$D_i^{Grt}\frac{\partial c}{\partial x}\bigg|_{x=0}^{Grt} = D_i^{Cor}\frac{\partial c}{\partial x}\bigg|_{x=0}^{Cor}$$

at a general mass balance (M). The equation for an atom of an isomorphically replaced component at a unit cross section will acquire the form:

$$-\int_0^t D_i^{Grt}\frac{\partial c(0, t)}{\partial x}dt = M = -\int_0^t D_i^{Cor}\frac{\partial c(0, t)}{\partial x}dt.$$

Now, if individual compositions from the diffusion profile are plotted in a diagram in terms concentration v. distance (c–x in Figs. 6 and 9), the area between the concentration axis, the $c_i(x) = X_{Mg}$ function, which was chosen to approximate the distribution of contents (magnesium numbers) along the diffusion profile, and the line for the initial equilibrium concentration c_0 is also proportional to the amount of matter that was

added (or extracted) by diffusion through a unit section during a time period of t, i.e.,

$$M = -\int_0^t D_i \frac{\partial c(0, t)}{\partial x} dt = \int_0^L [c_t(x) - c_0]\, dx. \quad (1)$$

In fact, this means that the ratios of respective areas in the plots are the same as the ratios of the mineral mole volumes in the diffusion pairs recalculated for one atom of an isomorphically exchanged component, for example:

$$Grt : Crd : Bt \approx (114/3) : (223/2) : (152/3) \approx 1 : 3 : 1.3.$$

The magnesium and iron interdiffusion proceeds much slower in a garnet lattice than in other minerals. Because of this, relatively large garnet grains usually retain their initial equilibrium concentrations c_0. This concentration is 0.18 in our sample. As is evident from the concentration plots in the cordierite and biotite, condition (1) is met if the biotite magnesium mole fraction was 0.44 instead of 0.50, and that of the cordierite was 0.59 instead of 0.60. This will be apparent if the $c_t(x)$ function is integrated (graphically or analytically) in compliance with equation (1) for each of the minerals. Insertion of the computed analytical dependencies from the plots into equation (1) yields:

$$M_{Mg}^{Grt} = \int_0^L [c_t(x) - c_0]\, dx = \int_0^{125} [X_{Mg}^{Grt} - c_0^{Grt}]\, dx$$

$$= \int_0^{125} [0.0924(x)^{0.138} - 0.18]\, dx = -2.7 \text{ conv.un}$$

(the minus sign indicates that magnesium is diffusionally extracted from the garnet, the integration limits are presented in micrometers). Analogous equations for the cordierite and biotite are:

$$M_{Mg}^{Crd} = \int_0^{500} [X_{Mg}^{Crd} - c_0^{Crd}]\, dx$$

$$= \int_0^{500} [0.694(x)^{-0.026} - 0.59]\, dx = 8.1 \text{ conv.un},$$

$$M_{Mg}^{Bt} = \int_0^{60} [X_{Mg}^{Bt} - c_0^{Bt}]\, dx$$

$$= \int_0^{60} [0.51 - 0.44]\, dx = 4.2 \text{ conv.un}.$$

As can be readily noticed, the calculated ratio of the integrated areas is similar to the theoretical ratio of the mineral molar volumes:

$$M_{Mg}^{Grt} : M_{Mg}^{Crd} : M_{Mg}^{Bt} = (2.7) : (8.1) : (4.2) = 1 : 3 : 1.5.$$

Such computations can be employed to estimate the extent to which a diffusion system was distorted (lack of mass balance), and to calculate equilibrium mineral compositions if they have been obliterated by a protracted retrograde process.

Hence, the small biotite grain near the garnet has substantially changed its composition, and its initial equilibrium magnesium mole fraction was similar to that of the matrix biotite. The cordierite rim is relatively thick, and its composition in the rear portions has almost remained the same. This composition can be used to calculate the metamorphic P–T conditions.

ESTIMATES OF THE METAMORPHIC P–T CONDITIONS

A logical implication of the diffusion model is that, generally, the obtained equilibrium compositions of the minerals must not reflect the peak metamorphic conditions (although we cannot rule this out in some instances). They should at least reflect a temperature T_0 at which the component redistribution became nonequilibrium. It is implied that, above this temperature, the diffusion rate was high relative to the cooling rate of the system, which was able to reestablish its thermodynamic equilibrium. Naturally, information on all high-temperature equilibria was lost.

The temperature was evaluated by well-calibrated equilibria (III and IV) with garnet, cordierite, and biotite (Perchuk *et al.*, 1983). It is reasonable to evaluate the pressure using two independent continuous reactions: one with sillimanite and cordierite [reaction (II)], and the other with sillimanite and plagioclase, both in assemblage with garnet:

$$Grs + Sil + Qtz = An, \quad (V)$$

corrected for the contents of grossular and spessartine in the garnet (Aranovich and Podlesskii, 1989). It is pertinent to note that assessments of the minimum P–T conditions on the basis of marginal compositions is quite arbitrary, because the very extreme compositions cannot be measured by a microprobe, and the compatible pressure evaluations on the basis of continuous reactions require that the respective reactions were proved to occur simultaneously in a closed system. It is useful to calculate metamorphic conditions using the *TPF* software package developed at the Institute of Experimental Mineralogy, Russian Academy of Sciences (Fonarev *et al.*, 1991). The P–T estimates yielded by consistent thermometers and barometers with independent calculation procedures for temperature and pressure seem to be the most realistic. Table 5 lists the thermodynamic evaluations (Perchuk *et al.*, 1983; Perchuk *et al.*, 1984; Aranovich and Podlesskii, 1989). Each of the lines (no.) presents the numbers of mineral analyses from Tables 1 - 4 (in line with Fig. 3) that were used to calculate equilibrium P–T conditions.

By virtue of the above-mentioned facts, the temperature and pressure estimates that were obtained using

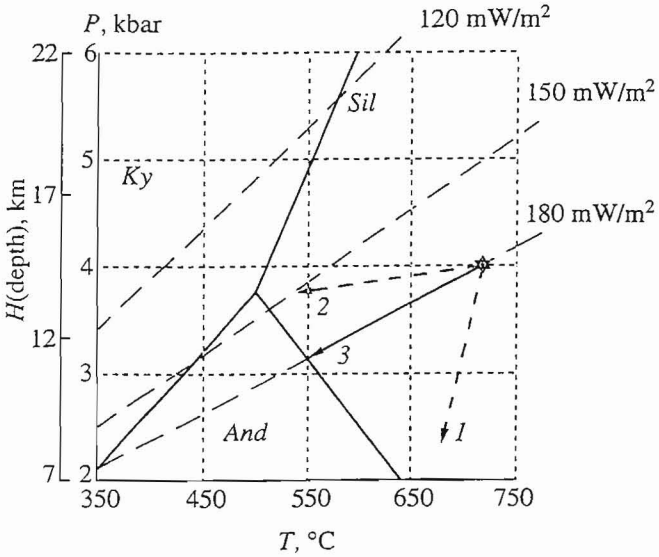

Fig. 10. Metamorphic evolution of the Voronezh Massif. Shown are the stability fields of aluminium silicates (*Ky, Sil,* and *And*) and isolines of constant heat fluxes (geotherms). The arrows indicate hypothetical variants of the retrograde evolution (see text for details): *1* – isothermal decompression, *2* – isobaric cooling, *3* – uplift along geotherms. The peak metamorphic conditions are estimated at 4 kbar and approximately 730°C using the *Grt–Crd* thermometer (asterisk in the plot). The trend passes from the geotherm with a heat flux of 180 mW/m² (geothermal gradient of about 50°C/km). If the initial cooling rate was 3°C/Ma, the uplift rate was approximately 0.03 km/Ma and the uplift time was 0.5 Ga for a depth of $H = 15$ km.

heat source degradation]. The grade of reversibility of the mineral systems depends on their cooling rates. If the rate if low, the system evolves in equilibrium, and its high-temperature assemblages grade into low-temperature parageneses. For example, the magnesium mole fractions of the garnet and cordierite should simultaneously increase due to the decomposition of the latter mineral according to reaction (II) at the very beginning of the retrograde evolution; later, staurolite, kyanite, chlorite, etc. would occur. The rocks in question carry no such features and, hence, their cooling rate was fairly high and the mass transfer in the system terminated very quickly.

RATE OF THE THERMAL EVOLUTION OF THE SYSTEM

Our detailed diffusion profiles with a good reproducibility (Figs. 6 and 7) provide a basis for calculating the cooling rate of the metamorphic system. The profiles utilize 190 individual microprobe analyses (for ten elements) and calculated cation proportions (which are not listed in this paper because of their large volume). The plots demonstrate the dependence of the magnesium mole fraction of the garnet solid solution on distance. The diffusion profile in the garnet at the contact with biotite is best preserved and can be used as a standard to calculate the cooling rate.

The computer numerical simulation of the diffusion zoning was performed using the *RC* software by Gerasimov (1992). The input parameters were: the enthalpy of exchange reaction (IV) $\Delta H^0 = 7844$ cal, the temperature at which the nonequilibrium exchange began $T_0 = 670$°C, the diffusion activation energy $Q = 82460$ cal, the preexponential factor $D_0 = 1.662$ cm²/sec, the initial equilibrium magnesium mole fraction of the garnet $X^{Bt}_{Mg} = c_0 = 0.18$, and the equilibrium magnesium mole fraction of the biotite $X^{Bt}_{Mg} = 0.44$.

The diffusion zoning was modeled over a wide range of cooling rates, from $s = 0.1$°C/Ma to $s = 100$°C/Ma. Figure 11 presents the calculated curves. The best fitness was observed between the reference profile and the curve for $s = 3$°C/Ma, and, considering the high fluctuation background, the function acquires the final form of $s = 3\ (^{+2}_{-1})$ °C/Ma. It is noteworthy that similar results were obtained for metapelites from central Finland, from the Svekofennian (Early Proterozoic) segment of the Baltic Shield (Lindstrom *et al.*, 1991). Furthermore, cooling rates of the same order are most often used in the calculations of the closure temperatures of K–Ar systems in isotopic thermochronology (Berger and York, 1981).

In order to best visualize the scale on which the mass transfer occurred during the retrograde evolution without the growth and dissolution processes (hydrothermal alterations, metasomatism, etc.), let us consider a temperature *v.* time function (Fig. 12), and compare two isothermal sections at 670°C and 470°C (i.e., the limits of the petrologically significant temperature interval). It follows from the model plot that the temperature had declined by 200°C for a time period of approximately 100 Ma, the cooling rate diminished by a factor of two, and the volume diffusion coefficient in garnet decreased by a factor of approximately 140 000. Let us choose a specific time interval over which the process can be considered isothermal. For example, the temperature diminished by only 3°C for 1 Ma at a temperature of 670°C (because $s = 3$°C/Ma). This case can be described using an isothermal approximation to evaluate the average square distance of a diffusion atom transfer in the form of a parabolic function:

$$x^2 \approx kDt.$$

If a certain amount of magnesium had diffused into the garnet for 1 Ma at 670°C, a similar mass transfer can be achieved at 470°C for 140 Ga, as it follows from the ratio of the respective diffusion coefficients ($D^{670}/D^{470} \approx 140\,000$). This means that, even if the cooling regime changed and the metamorphic complex had rested at 470°C for a few billion years, this would not introduce any distortion in the diffusion exchange between the minerals (the exchange had been completed by that

time). Hence, concerning the thermal regime, the diffusion profile carries information on the cooling dynamics mainly within the first hundred degrees of its temperature evolution from the moment of the system closure. The rest of the trend is a model extrapolation and only illustrates the general tendency in the monotonous cooling. In this connection, the linear portion of the plot near the point $T_0 = 670$°C is the most interesting, because this temperature best characterizes the geothermal regime during the first few million years of the retrograde evolution. On the one hand, this serves merely as a model restriction, but on the other, this attaches necessary correctness to the study.

CONCLUDING INTERPRETATION

When the temperature evolution rate of the system was determined and no signs of either its isobaric cooling or subisobaric decompression were detected, the only scenario to be considered is subgeothermal uplift. This scenario implies that the heat flux through the platform block during the regional metamorphism changed relatively little, and the retrograde temperature evolution was generally controlled by the uplift. Such an uplift must be expressed in a P–T plot by a line exactly parallel to the line of a constant heat flux, i.e., a geotherm (Fig. 10). The starting point of the path is, according to thermobarometric estimates, T = 730°C and P = 4 kbar; that is, the approximate coordinates of the geotherm with a heat flux of 180 mW/m^2, whereas the current heat flux on ancient shields and platforms is 4–5 times lower (Lyubimova *et al.*, 1983).

Proceeding from the fact that the P–T path coincides with the line of a constant heat flux, and the initial cooling rate was 3°C/Ma, we can readily calculate the uplift rate (more specifically, its vertical component). It was approximately 0.03 km/Ma and, thus, an equilibrium uplift from a depth H = 15 km required at least 0.5 Ga. According to the model plot (Fig. 12), the temperature at a depth of 300 m (from which the sample was recovered in the drillhole) must decrease to 200°C. Naturally, this value is just a rough extrapolation; however, it definitely points to the fact that, at a substantially slower uplift (when a subisobaric tendency dominates), there would not be enough time to complete the uplift. It was terminated with the onset of the platform stage in the Phanerozoic and an ending of all active vertical displacements on the Voronezh Massif. All of these considerations count in favor of the subgeothermal scenario of the P–T evolution during the Early Proterozoic. However, the model does not rule out the occurrence of a subisobaric branch of the path during the late protoplatform evolution of the massif, which could be caused by the gradual diminishing of the heat flux.

From the viewpoint of isotopic thermochronology, one can expect that, at such low cooling rates, the K–Ar systems of biotite and feldspars will close at temperatures of 300 - 400°C and 200 - 300°C, respectively

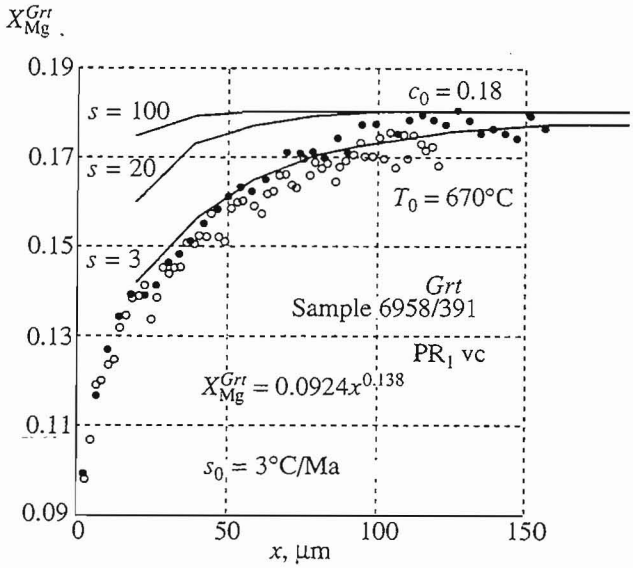

Fig. 11. Computer simulation of a retrograde diffusion zoning in garnet for the case of nonequilibrium exchange reaction with biotite.

The computed concentration curves for a variety of initial cooling rates (s) are presented in comparison with a natural compositional profile (microprobe data). The best fitting occurs at a cooling rate s = 3°C/Ma and a closure temperature T_0 = 670°C (biotite–garnet thermometer).

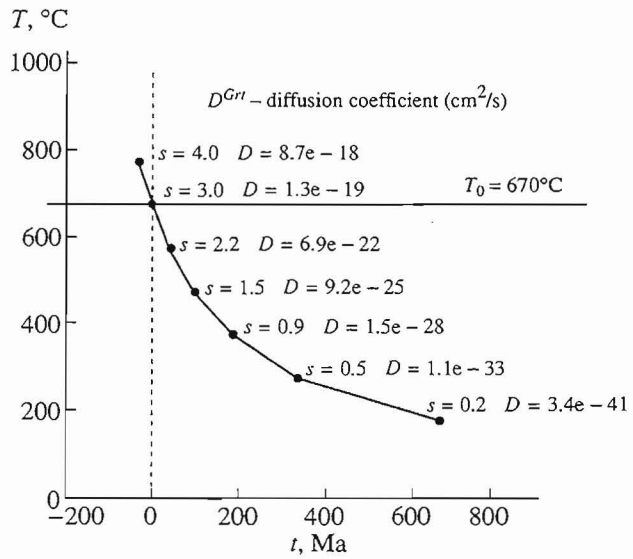

Fig. 12. Cooling dynamics of the Vorontsovskii (PR$_1$vc) metapelites, Voronezh Massif. Model approximation based on Sample 6958/391.

Within the linear portion of the plot over a temperature interval 670 - 370°C, the cooling rate has decreased by a factor of three for approximately 180 Ma; simultaneously, the diffusion rate in the garnet decreased by approximately a factor of one billion.

(Berger and York, 1981). In our case (Fig. 12), this implies that the time span separating the thermal event (metamorphic climax) and the "start" of the isotope watch (absolute age) can be as large as 200 - 300 Ma. Testing this conclusion will be a subject of later studies.

ACKNOWLEDGMENTS

The study was financially supported by the Russian Foundation for Fundamental Research, project no. 93-05-8034, and the International Science Foundation, grant M9P300.

REFERENCES

Aranovich, L.Ya. and Podlesskii, K.K., The Garnet + Sillimanite + Quartz = Cordierite Equilibrium: I. Experiment and Computations, *Miner. Zh.*, 1982, vol. 4, no. 1, pp. 20 - 32.

Aranovich, L.Ya. and Podlesskii, K.K., Geothermobarometry of High-Grade Metapelites: Simultaneously Operating Reactions, *Evolution of Metamorphic Belts*, Daly, J.S, Cliff, R.A., and Yardley, B.W.D., Eds., London: Geol. Soc. Spec. Publ., 1989, no. 43, pp. 45 - 61.

Berger, G.W. and York, D., Geothermometry from $^{40}Ar/^{39}Ar$ Dating Experiments, *Geochim. Cosmochim. Acta*, 1981, vol. 45, pp. 795 - 811.

Dodson, M.H., Closure Temperatures in Cooling Geochronological and Petrological Systems, *Contrib. Mineral. Petrol.*, 1973, vol. 40, no. 3, pp. 259 - 274.

Fonarev, V.I., Graphchikov, A.A., and Konilov, A.N., A Consistent System of Geothermometers for Metamorphic Complexes, *Int. Geol. Rev.*, 1991, vol. 33, no. 8, pp. 743 - 783.

Gerasimov, V.Yu., Experimental Study of Iron and Magnesium Interdiffusion in Garnet, *Dokl. Akad. Nauk SSSR*, 1987, vol. 295, no. 3, pp. 684 - 688.

Gerasimov, V.Yu., *Metamorphic Thermal Evolution and Reversibility of Mineral Reactions*, Moscow: Nauka, 1992.

Korikovskii, S.P., *Fatsii Metamorfizma Metapelitov* (Metamorphic Facies of Metapelites), Moscow: Nauka, 1979.

Lasaga, A.C., Geospeedometry: An Extension of Geothermometry, *Kinetics and Equilibrium in Geochemistry*, New York: Springer, 1983, vol. 3, pp. 81 - 114.

Lindstrom, R., Viitanen, M., Juhanoja, J., and Holtta, P., Geothermometry of Metamorphic Rocks: Examples in the Rantaasalmi-Sulkava and Kiuruvesi Areas, Eastern Finland, Biotite–Garnet Couples, *J. Metamorph. Geol.*, 1991, no. 9, pp. 181 - 190.

Lyubimova, E.A., Lyuboshits, V.M., and Parfenyuk, O.I., *Chislennye Modeli Teplovykh Polei Zemli* (Numerical Models for Earth's Thermal Fields), Moscow: Nauka, 1983.

Marakushev, A.A., *Problemy Mineral'nykh Fatsii Metamorficheskikh i Metasomaticheskikh Porod* (Mineral Facies of Metamorphic and Metasomatic Rocks), Moscow: Nauka, 1965.

Perchuk, L.L., *Ravnovesiya Porodoobrazuyushchikh Mineralov* (Equilibria of Rock-Forming Minerals), Moscow: Nauka, 1970.

Perchuk, L.L., Lavrent'eva, I.V., Aranovich, L.Ya., and Podlesskii, K.K., *Biotit–Granat–Kordieritovye Ravnovesiya i Evolyutsiya Metamorfizma* (Biotite–Garnet–Cordierite Equilibria and Metamorphic Evolution), Moscow: Nauka, 1983.

Perchuk, L.L., Lavrent'eva, I.V., Kotel'nikov, A.R., and Petrik, I., Comparative Characteristics of the Metamorphism Thermodynamic Regimes for Rocks of the Major Caucasian Range and the Western Carpathians, *Geol. Zbor. Geol. Carpathica*, 1984, vol. 35, no. 1, pp. 105 - 155.

Pollack, H.N. and Chapman, D.S., On the Regional Variation of Heat Flow, Geotherms, and Lithospheric Thickness, *Tectonophysics*, 1977, vol. 38, pp. 279 - 296.

Savko, K.A., Petrology of the Vorontsovskii Group Metamorphic Rocks, Voronezh Massif, *Cand. Sci. (Geol.–Miner.) Dissertation*, Moscow: Institute of Geology of Ore Deposits, Petrography, Mineralogy, and Geochemistry, Russian Academy of Sciences, 1991.